One-Dimensional Dynamics and Transport of DNA Molecules in a Quasi-Two-Dimensional Nanoslit

Po-Keng Lin,[†] Keng-hui Lin,[‡,§] Chi-Cheng Fu,[||] K.-C. Lee,[||] Pei-Kuen Wei,[§] Woei-Wu Pai,[⊥] Pei-Hsi Tsao,[†] Y.-L. Chen,*[,‡,§] and W. S. Fann*[,†,||,#]

Department of Physics, National Taiwan University, Taipei 10617, Taiwan, Republic of China; Institute of Physics, Research Center for Applied Sciences, and Institute of Atomic and Molecular Science, Academia Sinica, Taipei 11529, Taiwan, Republic of China; and Center for Condensed Matter Sciences and Institute of Polymer Science and Engineering, National Taiwan University, Taipei 10617, Taiwan, Republic of China

Received September 16, 2008; Revised Manuscript Received November 15, 2008

ABSTRACT: We report an unusual phenomena of attraction between DNA and the sidewall of a two-dimensional (2d) glass nanoslit with height, h, less than the Kuhn length l_K. The DNA molecules are stretched and diffuse along the wall. The scaling analysis reveals that the wall-bound DNA molecules exhibit one-dimensional (1d) diffusion. A modified blob model is able to predict the chain extension down to 30 nm, well into the subpersistence length regime where the chain deflection length should be considered. This discrepancy may be due to the partially bound confinement of chains near the sidewall. In contrast, the scaling analysis of DNA molecules far from the sidewall exhibit 2d dynamics that can be described by de Gennes and Odijk model for $h > l_K$ and $h < l_K$, respectively. We further apply the unusual wall attraction to trap and stretch DNA molecules around posts in a nanoslit. We demonstrate that the DNA molecules exhibit trapping−escaping movement, and they can be transported from post to post with an electric field.

1. Introduction

In the past few years there has been an unprecedented advance in micro- and nanofluidic systems. This has led to applications in DNA separation,[1−3] sequencing and mapping,[4] and advance fundamental research on polymer dynamics. Many popular microfluidic devices employ the electric field to transport DNA, strong confinement to stretch DNA, and collision barriers to separate DNA molecules by length.

Recent advances in nanofluidic fabrication technology allow scientists to create well-defined structures at the length scale comparable to the Kuhn length l_K (≈100 nm) of double-stranded DNA (ds-DNA) and to study polymer dynamics in confined geometry.[5−17] Single DNA molecules are shown to move freely in nanochannels[5] and rectangular nanoslits[9,16] as small as 30 nm. When the restricted dimension is larger than l_K, the chain conformation and dynamics can be described by the classical blob model.[18,19] When the restricted dimension is comparable to or less than l_K, the bending stiffness of polymer is affected by the confinement, as suggested by Odijk.[20] For such chains, the contributions from the restricted conformation entropy and the energy from polymer−wall interaction become significant. The complex interplay between the effects of confinement, hydrodynamic interactions, electrostatic interaction, and the entropy of solute and solvent particles may result in complex, counterintuitive dynamics as has been found in colloidal systems.[21,22]

As an example, Krishnan et al. observed a very unusual DNA dynamics near the wall in nanoslits, where classical theory expects chain depletion due to restricted chain conformational entropy. Instead, DNA molecules spontaneously adsorb and stretch along the wall in a two-dimensional slit of several microns in width and less than 100 nm in height.[23,24] Similar DNA−surface interaction induced stretching along a grooved cationic lipid membranes surface[25] has also been reported. However, a quantitative analysis is lacking. In this work, we investigate the conformation of DNA molecules in quasi-one-dimensional (Q1d) and quasi-two-dimensional (Q2d) environments and compare it with the predictions of de Gennes' blob model and Odijk's deflection length model. The Q2d environment is created by confining DNA molecules between two walls with separation h smaller than the radius of gyration (R_g) of DNA molecules. The Q1d environment is found, surprisingly, not by a square nanochannel with four walls but by an anomalous adsorption of DNA onto the sidewall adjoining to two parallel walls with $h < 140$ nm. In the first part of this work, we systematically investigate the chain extension, shape, and dynamics of individual ds-DNA molecules, confined in a wide rectangular nanoslit with slit height h from 20 nm (≈l_K/6) to 780 nm (≈6l_K), near and far away the sidewall of nanoslit.

We also investigate the potential application of electric field-driven collision and adsorption between DNA and fixed obstacles for DNA stretching[26] and separation[27] in nanofluidic chips. We designed a micropost array in the nanoslit to investigate DNA transport through the post arrays under an electric field. The mechanisms of the DNA collision with single cylindrical microheight post with radius of post close to the radius of gyration R_g of DNA exhibits a hooking process like the classical motion of rope-on-pulley.[26] In the nanoslit confinement, a micropost can act as a ring-shaped potential that traps DNA. We can electrically manipulate the trapped DNA transport in the ring-shaped trap arrays and compress−decompress DNA by switching on/off the electric field. This technique could be a powerful tool for studying multistep biochemical reaction at the single molecules level.

2. Blob Theory of Polymer in Confined Geometry

For a DNA molecule with contour length L confined in a square channel or a slit with channel dimension less than the DNA R_g, its chain extension r scales with the channel height h

* To whom correspondence should be addressed.
[†] Department of Physics, National Taiwan University.
[‡] Institute of Physics, Academia Sinica.
[§] Research Center for Applied Sciences, Academia Sinica.
[||] Institute of Atomic and Molecular Science, Academia Sinica.
[⊥] Center for Condensed Matter Sciences, National Taiwan University.
[#] Institute of Polymer Science and Engineering, National Taiwan University.

10.1021/ma8021037 CCC: $40.75
Published on Web 02/10/2009

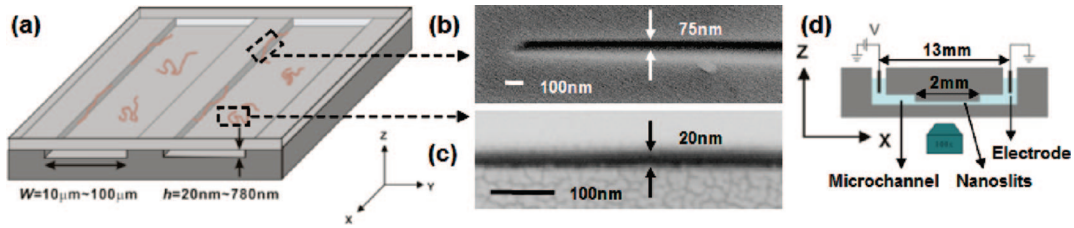

Figure 1. Design and the surface morphology of the nanofluidic chip. (a) Schematic drawing of the trapped DNA in a wide rectangular nanoslit. (b) Cross-sectional SEM image of wide rectangular nanoslit sidewall with $h = 75$ nm. (c) Region far from the sidewall with $h = 20$ nm in another nanoslit. (d) Schematic representation of the cross section for sealed fluidic channel. The dimensions between reservoir and length of nanoslit are 13 and 2 mm, respectively.

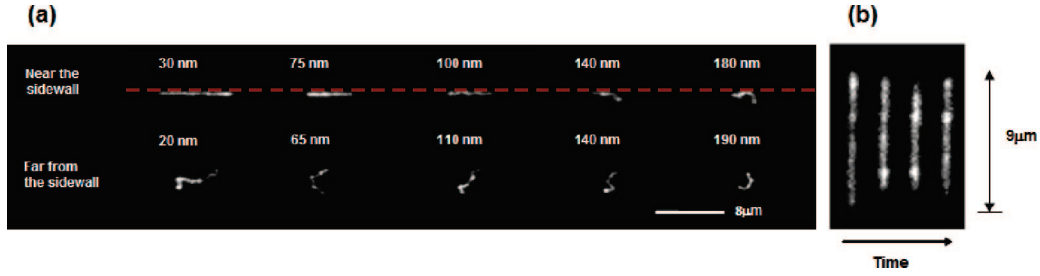

Figure 2. (a) Micrographs of DNA near the sidewall (the top column) and far from the wall (the bottom column). The length above each DNA denotes the height of the slit where the DNA is located. (b) Time series fluorescence images for λ-DNA trapped by the sidewall of nanoslit with $h = 30$ nm at a time interval of 0.4 s.

as[19] $r \sim h^{\nu}$, where the scaling component ν depends on the channel geometry. The blob theory predicts $\nu = -2/3$ in one-dimensional (1d) confinement and $\nu = -1/4$ in two-dimensional (2d) confinement.[19] Recent studies show that when a ds-DNA with persistence P is restricted in a channel smaller than its radius of gyration in bulk $R_{g,bulk}$, its statistical mechanical properties alter from the bulk to weak confinement ($R_{g,bulk} \gg h \gg P$), which is explained by the blob theory.[9,11,12,16] In the case where the channel height $h \ll P$, Odijk has developed a theory that takes into account that the chain segments are deflected by the confining walls.[20] The theory is further generalized by Burkhardt to the rectangular nanoslit with channel width D and height h.[28] Using the approximation that the average deflection angle is small, the relative extension can be expressed as[29]

$$\frac{r}{L} = 1 - 0.085\left[\left(\frac{D}{P}\right)^{2/3} + \left(\frac{h}{P}\right)^{2/3}\right] \quad (1)$$

However, the approximation of small deflection angle is most accurate when $r/L \approx 1$, and it becomes less accurate as (D/P) or (h/P) becomes large, i.e., as r/L approaches $R_{g,bulk}/L$.

3. Materials and Methods

3.1. Fabrication of Nanofluidic Devices. Figure 1a shows the schematic representation of device geometry used in the present study, which is a wide rectangular nanoslit with the width $D = 10-100$ μm and the height varying from 20−780 nm. The device is made by first patterning Pyrex 7740 glass wafers with photolithography, then etching the glass to the desired depth through inductive reactive ions etch (RIE) with CF_4 gas, and finally thermally fusing with a 0.17 mm Pyrex 7740 cover glass at 650 °C.[30] The cross-section SEM pictures of two pure slit devices with different heights, 75 and 20 nm, are shown in parts b and c of Figure 1, respectively. The SEM picture shown in Figure S1a of the Supporting Information indicates that the height of the nanoslit devices is uniform. Thus, we can rule out the possibility that the trapping is due to the collapse of the cover glass at the center of the channel and pushing the DNA toward the boundary region.

3.2. DNA Preparation. λ-DNA ($N = 48.50$ kbp, New England BioLabs) is used in these studies. The DNA buffer solution has 1/2 TBE (45 mM tris base, 45 mM boric acid, and 1 mM EDTA) with 10 mM sodium chloride (NaCl). The ionic strength and Debye length λ_D of the buffer solution are ≈35 mM[31,32] and ≈2 nm, respectively. DNA molecules are labeled with the fluorescent dye YOYO-1 (Molecular Probes) at a ratio of four base pairs per dye. The contour length and persistence length of λ-DNA are $L = 22$ μm and $P = 67$ nm after labeling.[33−35] The image buffer contains 0.1% pop-6 (v/v) (Applied Biosystems), which can reduce the surface attraction to prevent the DNA sticking on surface, 3% 2-mercaptoethanol (v/v) (Sigma-Aldrich), 0.1% β-D-glucose (w/w) (Sigma-Aldrich), 10 μg/mL catalase (Roche), and 50 μg/mL glucose oxidase (Roche) in 1/2 TBE buffer with 10 mM NaCl. The viscosity η of the image buffer is 1.09 cP at 293 K.

3.3. Fluorescence Microscopy. DNA molecules are introduced into the nanoslit by an electric field after they are first loaded in the reservoir connected to the nanoslit (Figure 1d). Data collection begins 1 h after the electric field is applied so that DNA molecules are relaxed from the initial stretching. Fluorescence microscopy is performed with an Olympus IX70 microscope with a 100×, NA 1.35 oil immersion objective, illuminated with an argon 488 nm laser (Coherent Innova 90). Images are captured by EM-CCD (Andor DV887DCS-BV) with 10−70 ms exposure time. The longest relaxation time of the DNA molecules is much longer than the exposure time, and the images are captured without rotational averaging. Generally, 200 frames over a period of 20−300 s are recorded for each DNA depending on its extensional relaxation time. A shutter (LS3T2, Vincent Associates) is synchronized with CCD for uniform fluorescence images and to reduce photobleaching.

4. Results and Discussion

4.1. Channel Height Dependences of DNA Trapping by Nanoslit Sidewall. Figure 2a shows the conformation of the DNA molecules at different locations in a nanoslit, 20−190 nm in height. DNA molecules near and far from the sidewalls are distinguished by the distance, d_{DNA}, from the center of DNA to the nearest sidewall. Far from the wall ($d_{DNA} > 5$ μm), the DNA molecules are coiled and diffuse freely in the quasi-2d space; near the sidewall ($d_{DNA} < 5$ μm), the DNA molecules are physically adsorbed to the sidewall. The physisorbed DNA are stretched and fluctuate in a linear fashion (Figure 2b and Supporting Information video 1).

To understand the 1d-like behavior in the quasi-2d environment, we obtain the mass distribution function $\Psi(\mathbf{r})$ of a DNA molecule from the fluorescence images and characterize the size

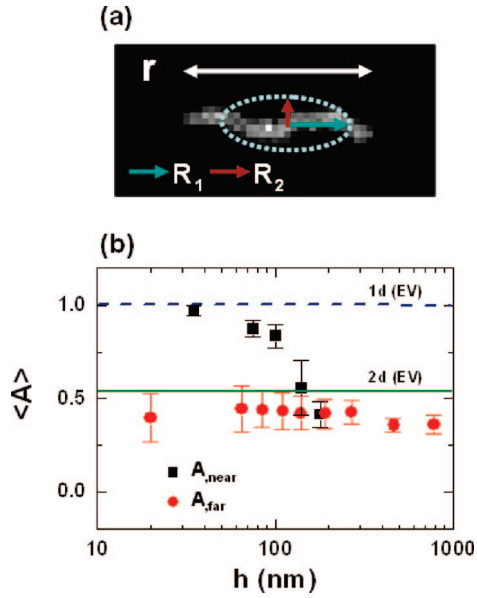

Figure 3. (a) λ-DNA image is represented by an ellipse with the characteristic length of the major R_1 and minor R_2 axes, calculated from the eigenvalues of the mass distribution function.[37] r is the extension of DNA. (b) Asphericity $\langle A \rangle$ is defined as $\langle (R_1^2 - R_2^2)^2/(R_1^2 + R_2^2)^2 \rangle$. The dashed line and the solid line are the values from the simulations of the self-avoiding walks (SAW) in 1d and 2d, respectively.

and shape of the molecule as illustrated in Figure 3a. The asphericity A measures the shape of a polymer, and its value ranges from 0 (spherical) to 1 (linear). The mean asphericity of DNA near and far from the sidewall are $\langle A_{near} \rangle$ and $\langle A_{far} \rangle$, respectively. Figure 3b shows $\langle A_{near} \rangle$ drops sharply from 0.97 to 0.41 when the height increases from 30 to 180 nm. The sharp drop indicates that the crossover of 2d-1d conformation for trapped DNA occurs for h between 100 and 140 nm, which is approximately equal to the Kuhn length. In contrast, $\langle A_{far} \rangle$ weakly increase with decreasing h, which suggests the projected shape becomes more anisotropic. This is consistent with a recent study of DNA shape confined in the nanoslit.[16] Simulations by Bishop and Saltiel have also shown that chain anisotropy increases as dimensionality decreases. They calculated $\langle A \rangle$ of 2d linear polymers with excluded volume (EV) to be 0.53.[36] The deviation from the theoretical value may be attributed to the limitation of our image resolution of ≈350 nm, leading to larger R_2 and smaller $\langle A_{far} \rangle$ observed than the simulation results. The average asphericity of the DNA in the nanoslit far from the wall is consistent with simulations of the 2d linear polymer with excluded volume.

Figure 4 shows the relationship between the measured relative extension of DNA molecules far from and near the sidewall versus the slit height h. We investigate the scaling exponent ν from $\langle r \rangle \sim h^{\nu}$ for DNA far from and near the sidewall. For DNA far from the sidewall, Figure 4a shows the scaling exponent of DNA extension is $\nu_{far} = -0.28 \pm 0.02$ for $h > 140$ nm. This follows from the blob scaling prediction in 2d ($\nu_{blob,2d} = -1/4$).[19] However, r_{far} exhibits a plateau when $h < 140$ nm. This implies that chain stiffness might play a role in polymer extension. Under strong confinement, the chain is deflected by the wall, and the blob picture no longer holds. In this "Odijk regime", the polymer exhibits the 2d "reflecting chain" conformation with the projected segment length $\lambda \cos\theta$ and the number of deflection segments $N_{Odijk} = L/\lambda$, where $\lambda \approx (h^2P)^{1/3}$, $\theta \approx h/\lambda$. For a chain confined below its l_K in a nanoslit, we may write the scaling law for its extension for $\theta = (h/P)^{1/3} \ll 1$ as

$$\begin{aligned} r &= (\lambda \cos\theta)\left(\frac{L}{\lambda}\right)^{3/4} \\ &= \left(1 - 0.5\left(\frac{h}{P}\right)^{2/3}\right)\left(\frac{h}{P}\right)^{1/6}\left(\frac{L}{P}\right)P \\ &= (C_1 h^{1/6} P^{1/12} - C_2 h^{5/6} P^{-7/12})L \end{aligned} \quad (2)$$

where $C_1 = (P/L)^{1/4} = 0.024$ and $C_2 = 0.5(P/L)^{1/4} = 0.012$, with $P = 67$ nm. Equation 2 has a maximum at $(h/P) = 0.25$, or H 17 nm, which suggests the lower bound of its validity and perhaps indicate the transition from quasi-2D to 2D conformation ($r/L = 0.28$ for λ-DNA). The dashed line in Figure 4a is the best fit with eq 2 using C_1* and C_2* as fitting parameters of r_{far} from $h = 20$ to 190 nm, where C_1* = 0.072 and C_2* = 0.020. The difference between the fitted and theoretical coefficients may be attributed to the varying degree of accuracy of the small deflection angle approximation in the regime of (h/P) fitted. Our measurements of r_{far} also agree with a recent study by Bonthuis et al. that showed R_g weakly depends on h when DNA confined in the Odijk regime.[16]

For DNA trapped near the sidewall region, the shape and dynamics of DNA are similar to confinement in a virtual rectangular nanoslit with the channel width D and height h. The blob theory predicts the relative extension with chain segment length $2P$ and effective width w_{eff} in rectangular nanoslit[38,39] is given by

$$\frac{r}{L} \approx \left(\frac{w_{eff}P}{Dh}\right)^{1/3} \quad (3)$$

For DNA in rectangular nanoslit, the exact transition from the blob (eq 3) to the Odijk regime (eq 1) is unclear. We have compared the measured r/L with both theories. It is straightforward to assign the virtual channel with a height equal to the device vertical dimension, while defining the width D of the channel for DNA physisorbed on the sidewall is ambiguous. From image analysis, we find that R_2 represents the conformational space sampled by the DNA in the horizontal plane perpendicular to the wall, corresponding to the virtual channel width. R_2 is observed to decrease with decreasing h, which implies the virtual channel width D depends on the h. Therefore, we assume a linear form $D = \gamma h$, where γ is a constant. Figure 4b shows that a fit using D with eq 3 is in good agreement with r_{near} ranging from $h = 30$ to 180 nm, with $w_{eff} = 4$ nm ($\approx 2\lambda_D$)[40] and $P = 67$ nm. The fit constant $\gamma = 6.03$ indicates $D = 180$ and 1080 nm for $h = 30$ and 180 nm, respectively. The dashed line in Figure 4b shows the fitting with Odijk picture (eq 1) in the range 75−180 nm. We optimized fitting with a constant $D = 1645 \pm 88$ nm. Within our experimental error bars, the Odijk model also agrees with the experiments except for the smallest 30 nm channel. Equation 1 predicts a weaker dependence of the relative extension on h. For near sidewall DNA molecules, the blob theory for 1d is in better agreement, suggesting that the chains are partly adsorbed onto the sidewalls and trapped in a 1d potential.

For DNA far from the sidewall, the transition from the blob to Odijk deflection chain behavior in the 2d nanoslit is clearly observed in Figure 4a. On the other hand, Figure 4b shows that the blob theory for 1d chains capture the growth of the relative extension as h decreases for DNA trapped near a sidewall. For DNA chains near a sidewall, the lack of a physical constraint in the virtual channel width most likely account for the lack of agreement with the Odijk theory due to the lack of a deflection length. This is in contrast to DNA molecules confined in a square nanochannel, where the Odijk predictions have been shown to agree with experiments.[5]

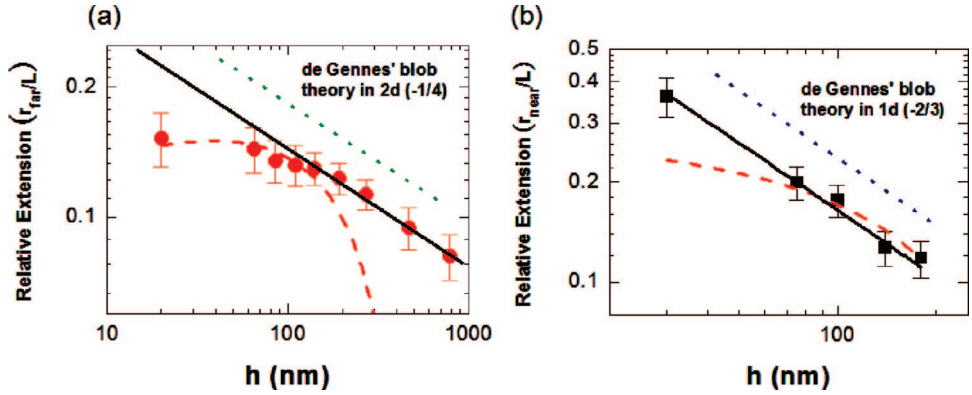

Figure 4. Log−log plot of relative extension r/L of λ-DNA far from (a) and near (b) the nanoslit sidewall as function as channel height h. The solid line indicates fit of eq 3. The dotted line in (a) and (b) are scaling predictions for chain extension in 2d ($\nu_{blob,2d} = -1/4$) and 1d ($\nu_{blob,1d} = -2/3$), respectively. The dashed line in (a) and (b) are the fits of eq 2 and eq 1, respectively.

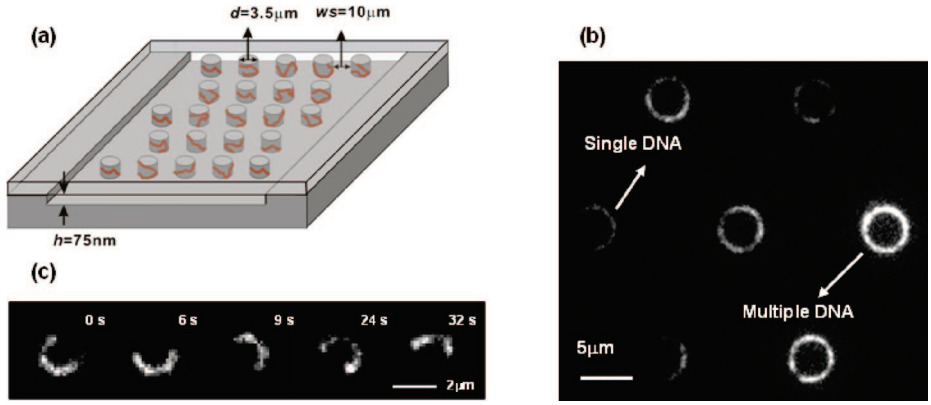

Figure 5. (a) Schematic drawing of the trapped DNA in the regular hexagonal cylinder arrays pattern in the nanoslit. (b) Fluorescence images of λ-DNA trapped and extended around single nanoheight post patterned in the nanoslit with $h = 75$ nm. A post can trap a large number of DNA molecules at the same time. (c) Time series fluorescence images for λ-DNA trapped by the sidewall of cylinder post with $h = 100$ nm.

4.2. Manipulating the Motion of Trapped DNA Using Electric Field. DNA trapping is also observed near cylindrical microposts in nanoslits. We take advantage of this phenomenon to trap DNA molecules near an obstacle in a thin nanoslit and transport them to other physical traps by using electric field. Figure 5a shows the schematic drawing of a device in which there is a micropillar array consisting of cylindrical posts, 3.5 μm in diameter, 10 μm in separation, and 75 nm in height (The AFM image is shown in Figure S1 of the Supporting Information.) Once the DNA molecules enter the device, they wrap around the post as shown in Figure 5b. A time lapse series of a DNA molecule that freely moves around a post is shown in Figure 5c and Supporting Information video 2.

When we apply a 390 V (300 V/cm) bias across two reservoirs, DNA molecules undergo translational motion along a channel at a speed of 8 μm/s, as shown in Figure 6a and Supporting Information video 3. When we apply the electric field to the device with micropillar arrays, the motion of DNA molecules depends on the strength of the electric field (Figure 6). In a weak field ($E < 400$ V/cm), the wall-bound DNA molecule is compressed into a tight blob at the stagnation point of the field (Figure 6b and Supporting Information video 4). In a stronger field ($E > 400$ V/cm), the DNA molecule is deformed from the blob at the stagnation point and then escapes the post with a stretched end. Then the DNA molecule hits the next micropost, wraps around the post in a stretched form, moves to the stagnation point in the compressed form, and then repeats the escape (Figure 6d and Supporting Information video 5). When the electric field is off, the DNA molecule relaxes from the compressed state to the physisorbed state. This decompression process is shown in Figure S2 and video 6 of the Supporting Information. We analyzed 35 compressed DNA after turning off the electric field and found the decompression time is 10.20 ± 3.05 s. The trapping−escaping process observed is very different from previously reported dynamics of DNA collision with a microheight post,[26] where the collision mechanism is dominated by repulsion between DNA and sidewall of microheight post that leads to hooking. In contrast, the trapping−escaping movement with nanoheight posts observed here is caused by the DNA−sidewall electrostatic attraction.[24] The mechanism here shares similarity to colloid transport in an array of optical traps.[41]

5. Conclusions

The interactions that cause the stretching and trapping of DNA with the nanoslit sidewall/post remain unclear. The DNA−wall attraction could be due to multiple factors. (1) The presence of multivalent ions in the buffer solution may lead to like charge attraction as found in polyelectrolyte condensation. (2) Entropic depletion of counterions between DNA and the wall may cause an effective entropic attraction between DNA and the wall. However, the length scale of counterion depletion is very short and requires the DNA to be within 1 or 2 counterion diameter (1 nm or less) of the wall. (3) Hindered chain relaxation near the sidewall due to stronger confinement constraint may lead to a prolonged nonequilibrium stretched chain that does not relax on the observation time scale. The sidewalls and the microposts could strongly hinder chain relaxation and lead to the impression that DNA molecules are "adsorbed" to the wall for a significant amount of time. Further theoretical and computational studies are needed to address these possibilities.

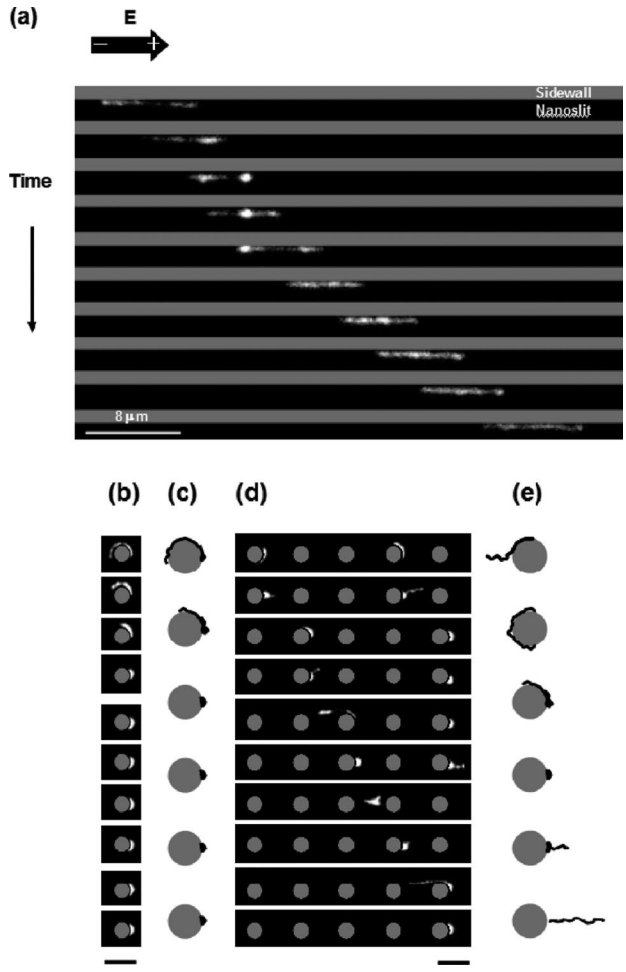

Figure 6. Manipulation of single DNA in nanoslit sidewall induced traps with electric field. (a) Time series fluorescence images of λ-DNA transport along the nanoslit sidewall ($h = 30$ nm) with time interval 0.5 s. (b) Time series fluorescence images of λ-DNA compression in the post-trap ($h = 75$ nm) under weak electric field ($E = 300$ V/cm) with time interval 1 s. (c) Schematic representation of compression process for post-trapped DNA under weak electric field. (d) Time series fluorescence image of λ-DNA transport through the posts patterned in 75 nm slit under strong electric field $E = 400$ V/cm with time interval 0.3 s. (e) Schematic representation of trapping−escaping process of single DNA transport in post-trapped arrays under strong electric field.

The post array patterned in the nanoslit forms a trap array for DNA molecules. The conformation of the molecules in this trap can be compressed and decompressed by switching on and off the dc E-field. The observation that an electric field may be used to collect DNA molecules at a field stagnation point could be very useful for step reactions for biochemical analysis. This post arrays device is able to trap and stretch DNA in nanoconfinement simultaneously. With this design, it is possible to perform multistep biochemical reactions to investigate the kinetics of DNA−protein interactions such as protein-induced DNA folding and restriction mapping by protein in confined environment. Our future work will focus on investigating the effects of surface charge and multivalent counterion on stretching and trapping of DNA.

Acknowledgment. We thank Dr. Pik-Yin Lai for insightful discussions. This research was supported by the Academia Sinica Nanoprogram and The National Science Council (Grant No. NSC 96-2112-M-002-035-MY3).

Supporting Information Available: Figures showing surface morphology of nanofluidic chips (Figure S1) and decompression of post-trapped compressed λ-DNA (Figure S2); movie files (videos 1−6). This material is available free of charge via the Internet at http://pubs.acs.org.

References and Notes

(1) Han, J.; Craighead, H. G. *Science* **2000**, *288*, 1026.
(2) Fu, J. P.; Yoo, J.; Han, J. Y. *Phys. Rev. Lett.* **2006**, *97*, 018103.
(3) Fu, J. P.; Schoch, R. B.; Stevens, A. L.; Tannenbaum, S. R.; Han, J. Y. *Nat. Nanotechnol.* **2007**, *2*, 121.
(4) Riehn, R.; Lu, M. C.; Wang, Y. M.; Lim, S. F.; Cox, E. C.; Austin, R. H. *Proc. Natl. Acad. Sci. U.S.A.* **2005**, *102*, 10012.
(5) Reisner, W.; Morton, K. J.; Riehn, R.; Wang, Y. M.; Yu, Z. N.; Rosen, M.; Sturm, J. C.; Chou, S. Y.; Frey, E.; Austin, R. H. *Phys. Rev. Lett.* **2005**, *94*, 196101.
(6) Reccius, C. H.; Mannion, J. T.; Cross, J. D.; Craighead, H. G. *Phys. Rev. Lett.* **2005**, *95*, 268101.
(7) Riehn, R.; Austin, R. H.; Sturm, J. C. *Nano Lett.* **2006**, *6*, 1973.
(8) Mannion, J. T.; Reccius, C. H.; Cross, J. D.; Craighead, H. G. *Biophys. J.* **2006**, *90*, 4538.
(9) Balducci, A.; Mao, P.; Han, J. Y.; Doyle, P. S. *Macromolecules* **2006**, *39*, 6273.
(10) Stein, D.; van der Heyden, F. H. J.; Koopmans, W. J. A.; Dekker, C. *Proc. Natl. Acad. Sci. U.S.A.* **2006**, *103*, 15853.
(11) Hsieh, C. C.; Balducci, A.; Doyle, P. S. *Macromolecules* **2007**, *40*, 5196.
(12) Lin, P. K.; Fu, C. C.; Chen, Y. L.; Chen, Y. R.; Wei, P. K.; Kuan, C. H.; Fann, W. S. *Phys. Rev. E* **2007**, *76*, 011806.
(13) Balducci, A.; Hsieh, C. C.; Doyle, P. S. *Phys. Rev. Lett.* **2007**, *99*, 238102.
(14) Reccius, C. H.; Stavis, S. M.; Mannion, J. T.; Walker, L. P.; Craighead, H. G. *Biophys. J.* **2008**, *95*, 273.
(15) Hsieh, C. C.; Balducci, A.; Doyle, P. S. *Nano Lett.* **2008**, *8*, 1683.
(16) Bonthuis, D. J.; Meyer, C.; Stein, D.; Dekker, C. *Phys. Rev. Lett.* **2008**, *101*, 108303.
(17) Strychalski, E. A.; Levy, S. L.; Craighead, H. G. *Macromolecules* **2008**, *41*, 7716.
(18) Brochard, F.; Degennes, P. G. *J. Chem. Phys.* **1977**, *67*, 52.
(19) Daoud, M.; Degennes, P. G. *J. Phys. (Paris)* **1977**, *38*, 85.
(20) Odijk, T. *Macromolecules* **1983**, *16*, 1340.
(21) Kepler, G. M.; Fraden, S. *Phys. Rev. Lett.* **1994**, *73*, 356.
(22) Crocker, J. C.; Grier, D. G. *Phys. Rev. Lett.* **1996**, *77*, 1897.
(23) Krishnan, M.; Monch, I.; Schwille, P. *Nano Lett.* **2007**, *7*, 1270.
(24) Krishnan, M.; Petráek, Z.; Mönch., I.; Schwille, P. *Small* **2008**, *4*, 1900.
(25) Hochrein, M. B.; Leierseder, J. A.; Golubovic, L.; Radler, J. O. *Phys. Rev. Lett.* **2006**, *96*, 038103.
(26) Randall, G. C.; Doyle, P. S. *Phys. Rev. Lett.* **2004**, *93*, 058102.
(27) Huang, L. R.; Tegenfeldt, J. O.; Kraeft, J. J.; Sturm, J. C.; Austin, R. H.; Cox, E. C. *Nat. Biotechnol.* **2002**, *20*, 1048.
(28) Burkhardt, T. W. *J. Phys. A* **1997**, *30*, L167.
(29) Jo, K.; Dhingra, D. M.; Odijk, T.; de Pablo, J. J.; Graham, M. D.; Runnheim, R.; Forrest, D.; Schwartz, D. C. *Proc. Natl. Acad. Sci. U.S.A.* **2007**, *104*, 2673.
(30) Mao, P.; Han, J. Y. *Lab Chip* **2005**, *5*, 837.
(31) Li, A. Z.; Qi, L. J.; Shih, H. H.; Marx, K. A. *Biopolymers* **1996**, *38*, 367.
(32) Dempsey, D. P. A. B. *Buffers for pH and Metal Ion Control*; Chapman and Hall: London, 1974.
(33) Makita, N.; Ullner, M.; Yoshikawa, K. *Macromolecules* **2006**, *39*, 6200.
(34) Perkins, T. T.; Smith, D. E.; Larson, R. G.; Chu, S. *Science* **1995**, *268*, 83.
(35) Baumann, C. G.; Smith, S. B.; Bloomfield, V. A.; Bustamante, C. *Proc. Natl. Acad. Sci. U.S.A.* **1997**, *94*, 6185.
(36) Bishop, M.; Saltiel, C. J. *J. Chem. Phys.* **1988**, *88*, 3976.
(37) Rudnick, J.; Gaspari, G. *Science* **1987**, *237*, 384.
(38) Turban, L. *J. Phys. (Paris)* **1984**, *45*, 347.
(39) Reisner, W.; Beech, J. P.; Larsen, N. B.; Flyvbjerg, H.; Kristensen, A.; Tegenfeldt, A. J. O. *Phys. Rev. Lett.* **2007**, *99*, 058302.
(40) Marko, J. F.; Siggia, E. D. *Macromolecules* **1995**, *28*, 8759.
(41) Korda, P. T.; Taylor, M. B.; Grier, D. G. *Phys. Rev. Lett.* **2002**, *89*, 128301.

MA8021037